Published in final edited form as:
Biochemistry. 2011 November 15; 50(45): 9845–9856. doi:10.1021/bi2011306.

GRP1 PH Domain, Like AKT1 PH Domain, Possesses a Sentry Glutamate Residue Essential for Specific Targeting to Plasma Membrane PI(3,4,5)P_3

Carissa Pilling, **Kyle E. Landgraf**[^], and **Joseph J. Falke**[*]
Department of Chemistry and Biochemistry and the Molecular Biophysics Program, University of Colorado, Boulder, CO 80309-0215

Abstract

During the appearance of the signaling lipid PI(3,4,5)P_3, an important subset of pleckstrin homology (PH) domains target signaling proteins to the plasma membrane. To ensure proper pathway regulation, such PI(3,4,5)P_3-specific PH domains must exclude the more prevalant, constitutive plasma membrane lipid PI(4,5)P_2 and bind the rare PI(3,4,5)P_3 target lipid with sufficiently high affinity. Our previous study of the E17K mutant of protein kinase B (AKT1) PH domain, together with evidence from Carpten et al (1), revealed that the native AKT1 E17 residue serves as a sentry glutamate that excludes PI(4,5)P_2, thereby playing an essential role in specific PI(3,4,5)P_3 targeting (2). The sentry glutamate hypothesis proposes that an analogous sentry glutamate residue is a widespread feature of PI(3,4,5)P_3-specific PH domains, and that charge reversal mutation at the sentry glutamate position will yield both increased PI(4,5)P_2 affinity and constitutive plasma membrane targeting.

To test this hypothesis the present study investigates the E345 residue, a putative sentry glutamate, of General Receptor for Phosphoinositides 1 (GRP1) PH domain. The results show that incorporation of the E345K charge reversal mutation into GRP1 PH domain enhances PI(4,5)P_2 affinity 8-fold and yields constitutive plasma membrane targeting in cells, reminiscent of the effects of the E17K mutation in AKT1 PH domain. Hydrolysis of plasma membrane PI(4,5)P_2 releases E345K GRP1 PH domain into the cytoplasm and the efficiency of this release increases when target Arf6 binding is disrupted. Overall, the findings provide strong support for the sentry glutamate hypothesis and suggest that the GRP1 E345K mutation will be linked to changes in cell physiology and human pathologies, as demonstrated for AKT1 E17K (1, 3). Analysis of available PH domain structures suggests that a lone glutamate residue (or, in some cases an aspartate) is a common, perhaps ubiquitous, feature of PI(3,4,5)P_3-specific binding pockets that functions to lower PI(4,5)P_2 affinity.

Keywords

peripheral membrane protein; protein kinase B; pleckstrin homology domain; phosphatidylinositol-3,4,5-trisphosphate signaling; phosphoinositide

Signaling events at the cytoplasmic surface of the plasma membrane play a central role in a wide array of signaling cascades, and the signaling lipid PI(3,4,5)P_3 serves as an important second messenger at that membrane surface. Upon activation by upstream signals, the regulatory enzyme phosphoinositide-3-kinase (PI3K) phosphorylates the constitutive plasma

[*]To whom correspondence should be addressed: falke@colorado.edu, Tel (303) 492-3503, Fax (303) 492-5894.
[^]Current address: Early Discovery Biochemistry, Genentech, Inc., South San Francisco CA 94099

membrane lipid $PI(4,5)P_2$ to generate $PI(3,4,5)P_3$ (4–6). The resulting appearance of a $PI(3,4,5)P_3$ signal in the plasma membrane recruits an array of signaling proteins to the membrane surface. Typically these proteins possess a pleckstrin homology (PH) domain that specifically targets $PI(3,4,5)P_3$. Upon recruitment to the plasma membrane, such proteins are activated and regulate various essential cell processes including growth, chemotaxis, DNA synthesis, cytoskeletal rearrangements, vesicle trafficking, and apoptosis (4, 6–16).

Over 561 human proteins contain PH domains and a significant fraction of these PH domains are believed to bind PIP lipids with high affinity (17). PH domains that are recruited to the plasma membrane specifically during a $PI(3,4,5)P_3$ signaling event face a significant target recognition challenge: they must selectively bind $PI(3,4,5)P_3$, which is a rare membrane component, while excluding the constitutive plasma membrane $PI(4,5)P_2$ which is at least 100-fold more prevalent even during a peak $PI(3,4,5)P_3$ signal (4, 13).

PH domains share a common core structure consisting of two antiparallel β-sheets forming a β-sandwich (7, 18). At one edge of the β-sandwich up to three connecting loops provide basic side chains and other contacts that form the binding pocket for the negatively charged target lipid headgroup. The length and sequence of these loops provide each PH domain with its appropriate headgroup specificity (19) and, in principle, loop mutations could alter membrane recognition yielding dramatic cellular consequences. For example, Carpten et al. (1) found that the E17K mutation in the PH domain of the regulatory kinase AKT1 causes constitutive plasma membrane targeting, hyperactivation of AKT1 kinase, transformation of tissue culture cells. This mutation is linked to multiple human pathologies including cancers and Proteus syndrome (1, 3).

Our previous study of the E17K AKT1 PH domain revealed the mechanistic basis of its constitutive plasma membrane targeting, thereby uncovering a new molecular mechanism of carcinogenesis and leading to the sentry glutamate hypothesis of $PI(3,4,5)P_3$ specificity (2). For proper silencing of AKT1 kinase (also termed protein kinase B or PKB), it is crucial that the PH domain remain docked to its inhibitory site on the kinase domain until a $PI(3,4,5)P_3$ signal recruits the PH domain and relieves autoinhibition, thereby activating the kinase (20–23). Consequently, it is crucial that the PH domain exclude constitutive plasma membrane $PI(4,5)P_2$ to prevent kinase activation in the absence of a $PI(3,4,5)P_3$ signal. We found that the E17K mutation greatly enhances PH domain affinity for $PI(4,5)P_2$, thereby explaining its known biological effects (including constitutive plasma membrane targeting, kinase hyperactivation, cell transformation, carcinogenicity and tissue overgrowth (2)). In addition, we proposed that other $PI(3,4,5)P_3$-specific PH domains may also possess sentry glutamate residues.

The sentry glutamate hypothesis predicts that a glutamate-to-lysine charge reversal mutation at the sentry glutamate position of an arbitrary $PI(3,4,5)P_3$-specific PH domain will, like the AKT1 E17K mutation, both enhance $PI(4,5)P_2$ affinity and drive constitutive plasma membrane targeting (2). The present study tests this hypothesis by introducing the E345K charge reversal mutation at the putative sentry glutamate residue of General Receptor for Phosphoinositides 1 (GRP1). GRP1 is an Arf6 guanidine-nucleotide exchange factor (GEF) that catalyzes the activation of Arf6-GDP to Arf6-GTP at the plasma membrane surface. The GRP1 PH domain possesses a $PI(3,4,5)P_3$-specific binding pocket as well as an Arf6 binding site that includes residues I307 and K340 (Figure 1) (24, 25). Previous findings have concluded that Arf6 and $PI(3,4,5)P_3$ binding both contribute to plasma membrane affinity (25). The putative sentry glutamate residue of GRP1 PH domain, E345 (Figure 1), is located adjacent to the $PI(3,4,5)P_3$ headgroup binding pocket. Notably, the GRP1 E345 residue is found on a different loop and on the opposite side of the $PI(3,4,5)P_3$ inositol ring relative to the AKT1 E17 residue (18, 26, 27), but both glutamates are close enough to directly contact

the bound headgroup. The varying locations of putative sentry glutamates (see Discussion) is not surprising given the structural diversity of PH domain PI(3,4,5)P_3 binding pockets.

As predicted by the sentry glutamate hypothesis, the present findings indicate that the GRP1 E345K mutation increases PH domain affinity for PI(4,5)P_2 and triggers constitutive plasma membrane targeting. The effects of this mutation on PI(3,4,5)P_3 and PI(4,5)P_2 binding, both *in vitro* and in live cells, provide strong evidence that the native E345 side chain is a sentry glutamate ensuring minimal plasma membrane association until appearance of a PI(3,4,5)P_3 signal. More broadly, analysis of the available crystal structures of other PI(3,4,5)P_3-specific PH domains reveals analogous acidic side chains adjacent to the headgroup binding pocket that likely serve as sentry glutamate (or asparate) residues to decrease PI(4,5)P_2 affinity, thereby ensuring plasma membrane targeting and pathway activation occurs only during a PI(3,4,5)P_3 signal.

Materials and Methods

Reagents

All lipids were synthetic unless otherwise indicated. 1-Palmitoyl-2-oleoyl-*sn*-glycero-3-phosphocholine (phosphatidylcholine, POPC, PC); 1-palmitoyl-2-oleoyl-*sn*-glycero-3-phosphoethanolamine (phosphatidylethanolamine, POPE, PE); 1-palmitoyl-2-oleoyl-*sn*-glycero-3-phosphoserine (phosphatidylserine, POPS, PS); L-α-phosphatidylinositol natural from bovine liver; L-α-phosphatidylinositol-4,5-bisphosphate (PI(4,5)P_2, PIP_2) natural from porcine brain; and sphingomyelin natural from porcine brain were all purchased from Avanti Polar Lipids. 1,2-dipalmitoyl-phosphatidylinositol-3,4,5-trisphosphate (phosphatidylinositol-3,4,5-trisphosphate, PI(3,4,5)P_3) was from Cayman Chemical. N-[5-(Dimethylamino)naphthalene-1-sulfonyl]-1,2-dihexadecanoyl-*sn*-glycero-3-phosphoethanolamine (dansyl-PE, dPE) was from Molecular Probes. Cholesterol (CH), inositol-1,2,3,4,5,6-hexakisphosphate (IP_6) were from Sigma. Lipofectamine 2000 transfection reagent was from Invitrogen. Dithiothreitol (DTT) was purchased from Research Products International. Human recombinant PDGF-BB was purchased from PeproTech.

Preparation of Purified PH domains

For *in vitro* binding studies the PH domains of human GRP1 (residues 255–392) and mouse PLCδ1 (residues 12–142) were cloned by PCR as previously described into the EcoRI/XbaI site of a glutathione S-transferase (GST)-fusion vector (13). Mutagenesis of GRP1 PH was carried out using a QuickChangeXLII site directed mutagenesis kit (Stratagene). The GST-fusion constructs were overexpressed in BL21 *Escherichia coli* cells and isolated on a glutathione affinity column as previously described (13).

Preparation of Lipid Mixtures and Phospholipid Vesicles

Phospholipid bilayer vesicles were created using three lipid compositions (see Table 1) to mimic the plasma membrane inner leaflet either lacking or containing a PIP lipid: PM (−) PIP; PM (+) PI(4,5)P_2; and PM (+) PI(3,4,5)P_3. All lipids were dissolved in chloroform except PI(3,4,5)P_3, which was dissolved in chloroform/methanol/water (1/2/0.8). Subsequently, each given lipid mixture was created in the indicated mole ratios and dried under vacuum until all solvent was removed, then hydrated by vortexing with binding buffer (25 mM N-(2-hydroxyethyl)piperazine-N′-2-ethanesulfonic acid (HEPES) (pH 7.4 with KOH), 140 mM KCl, 15 mM NaCl, 0.5 mM $MgCl_2$). Finally, sonicated unilamellar phospholipids vesicles (SUVs) were prepared using a Misonix XL2020 probe sonicator as previously described (2, 13), yielding a total lipid concentration of 3 mM.

Fluorescence Spectroscopy

Equilibrium binding experiments were carried out on a Photon Technology International QM-2000-6SE steady state fluorescence spectrometer at 25°C in binding buffer (above) plus 10 mM dithiothreitol (DTT) as previously described (2, 13). Excitation and emission slitwidths were 1 nm and 8 nm, respectively. Wavelengths used for specific experiments are indicated below.

Quantitative Measurement of PIP Lipid Affinity and Specificity

Our previously described competitive displacement assay was used to quantitate the high affinity binding of each PH domain to the selected PIP lipids (2, 13). In this approach, soluble inositol-1,2,3,4,5,6-hexakisphosphate (IP_6) was employed as a competitive inhibitor to drive equilibrium displacement of PH domain from PIP-lipid containing membranes, while monitoring displacement by protein-to-membrane FRET. To determine the equilibrium dissociation constant for PIP lipid binding K_D (PIP_n) it was necessary to measure both the affinity of the free PH domain for the competitive inhibitor IP_6 as well as the competitive inhibition constant for IP_6 displacement of the PH domain from the target membrane.

The equilibrium dissociation constant of the free PH domain for the competitive inhibitor, K_D (IP_6), was measured using an increase in intrinsic Trp fluorescence to monitor binding of IP_6 to the protein. Increasing concentrations of IP_6 were titrated into a sample containing free PH domain protein (0.5 μM), 10mM DTT, and binding buffer. Intrinsic tryptophan fluorescence was measured using excitation and emission wavelengths λ_{ex} = 284 nm and λ_{em} = 322 nm (for GRP1 PH) or λ_{em} = 340 nm (for PLCδ1 PH). Sodium phosphate, at six times the corresponding IP_6 concentration, was also added to a control sample that was run parallel to the sample experiments to determine the effect of a highly anionic molecule on the Trp emission. The raw data was then corrected for dilution and the control cuvette data was subsequently subtracted, yielding the final titration data. Finally, a nonlinear least square curve fit employing Eq. 1 determined the equilibrium dissociation constant for IP_6 [($K_D(IP_6)$]:

$$F=\Delta F_{max}\{[IP_6]/(K_D(IP_6)+[IP_6])\}+C \quad (1)$$

where F is the observed fluorescence at a given IP_6 concentration [IP_6] and ΔF_{max} is the total magnitude of the fluorescence change at saturation with IP_6.

The equilibrium apparent inhibition constant, $K_I(IP_6)_{app}$, was measured by titrating IP_6 into a sample containing the PH domain bound to a membrane-associated PIP lipid, using a protein-to-membrane FRET assay to monitor the membrane-bound PH domain. The solution contained 0.5 μM PH domain, 10 mM DTT, 3 μM accessible PIP lipid, 300 μM total lipid, and binding buffer. The IP_6 competitively displaces the PH domain from the membrane, yielding a decrease in FRET. IP_6 was also added to a control sample that was run parallel to the sample experiments to determine the effect of free IP_6 on the FRET emission of free membranes. The control sample contained 10mM DTT, 3 μM accessible PIP lipid, 300 μM total lipid, and binding buffer. The raw data was corrected for dilution and then the control was subtracted from each sample. Finally, a nonlinear least square curve fit utilizing Eq. 2 determined the equilibrium apparent inhibition constant for IP_6 [($K_I(IP_6)_{app}$]:

$$F=\Delta F_{max}(1-\{[IP_6]/(K_I(IP_6)_{app}+[IP_6])\})+C \quad (2)$$

where F is the observed fluorescence and ΔF_{max} is the total magnitude of the fluorescence change at saturation with IP_6. Using the (K_D (IP_6)) and (K_I (IP_6) $_{app}$) and employing Eq. 3 the desired equilibrium dissociation constant for the binding of the PH domain to the membrane-associated PIP lipid (K_D (PIP_n)) was deduced:

$$(K_I(IP_6)_{app}=(K_D(IP_6)\,[\,1+\{[PIP_n]_{free}/K_D(PIP_n)\}] \quad (3)$$

For additional details see our previous publications (2, 13).

Quantitative Measurement of Association and Dissociation Kinetics

All kinetic experiments were carried out using Applied Photophysics SX.17 stopped-flow fluorescence instrument to monitor changes in protein-to-membrane FRET induced by membrane association or dissociation, always in binding buffer plus 10 mM DTT, at 25°C as previously described (2, 13). Association kinetics were measured by rapidly mixing PH domain (0.5 μM) with SUVs (300 μM total lipid) containing excess PIP_n target lipid (3 μM accessible). Under these conditions the forward binding reaction is virtually irreversible due to the high affinity of the PH domain for PIP lipid, and best fit analysis of the binding timecourse with a double exponential yielded a predominant, fast component used to calculate the on-rate constant (k_{on}). Dissociation kinetics were measured by rapidly mixing preformed, PH domain-membrane complex (0.5 μM protein, 300 μM total lipid) with excess IP_6 (10 mM for GRP1 WT PH domain with PIP_3; 20 mM for GRP1 E345K or E345K/I307A PH domain with PIP_3; 8 mM for GRP1 E345K or E345K/I307A or PLCδ1 PH domain with PIP_2). Best fitting of a double exponential function to the dissociation timecourse typically yielded fast and predominant slow components, and the latter was used to calculate the off-rate constant (k_{off}) as previously described (13).

Fluorescent Fusion Proteins

The pEGFP-GRP1 PH construct was a kind gift to our lab from Ben Tycko (Columbia University Medical Center, New York) (28), and pRFP-PLCδ1 PH was a kind gift from M. Katan (Cancer Research UK Centre for Cell and Molecular Biology, London). In each plasmid, the fluorescent protein was replaced with Citrine fluorescent protein (Cit) by subcloning. Mutagenesis of Cit-GRP1 PH to generate the indicated mutations was carried out using a QuickChangeXLII site directed mutagenesis kit (Stratagene).

Transfections into Live Cells

NIH 3T3 cells (American Type Culture Collection) were cultured in DMEM containing 10% fetal bovine serum, 100 U/ml penicillin, 100 μg/ml streptomycin, 0.292 mg/ml glutamine in 5% CO_2 at 37°C. Cells were plated in 6 cm culture dishes at 4.2×10^5 cells/dish and let sit overnight. Transfections were carried out with 4 μg total DNA using lipofectamine 2000 (Invitrogen) with OptiMEM (Invitrogen) according to manufacturer's protocol. Prior to imaging, transfected cells (24–48 hours after transfection) were plated in 35 mm glass bottom dishes (MatTek) at 1×10^5 cells/dish and adhered for one to two hours. Where indicated, serum starvation of cells was carried out in DMEM containing 0.2% BSA and 0.292 mg/ml glutamine and incubated for 6 hours in 5% CO_2 at 37°C.

Cell Imaging Studies

Transfected NIH 3T3 cells were rinsed and incubated in HBSS buffered with 25 mM HEPES at pH 7.4 (HHBSS) containing 0.01% endotoxin-free BSA. In experiments involving Ca^{2+}-stimulated $PI(4,5)P_2$ hydrolysis by phospholipase C, the HBSS was purchased Ca^{2+}- and Mg^{2+}-free and subsequently supplemented with 0.493 mM magnesium

chloride and 0.407 mM magnesium sulfate to provide an initial Ca^{2+}-free extra cellular environment. Immediately prior to imaging, ionomyosin was added to 10 μM. Subsequently, at time zero Ca^{2+} was added at the indicated extracellular concentration to trigger Ca^{2+} influx as previously described (2, 29, 30). Citrine images were acquired on a Nikon inverted microscope equipped with a 60 × 1.4 N.A. oil immersion objective, a CFP/YFP-Cit/RFP dichroic mirror, single band excitation and emission filters (Chroma Technology), a CoolSNAP ES camera (Photometrics), and a mercury lamp. For the kinetic time courses, time-lapse imaging involved 300 msec acquisitions with a total of 30 sec between image sets analyzed in ImageJ (NIH, http://rsb.info.nih.gov/ij/).

Results

Strategy and PH Domains Employed

The present study of the putative sentry glutamate E345 of GRP1 began with the construction of a set of PH domains possessing side chains of varying charge at the 345 position. Our previous study (2) of the AKT1 sentry glutamate E17K employed three sentry position variants: E17(WT), E17Q and E17K. To facilitate comparisons with this previous study we constructed and isolated the corresponding three GRP1 PH domains: E345(WT), E345Q and E345K. The relative affinities of these three GRP1 PH domains for membrane-bound PI(3,4,5)P_3 and PI(4,5)P_2, each embedded in bilayers mimicking the lipid composition of plasma membrane, were initially measured in a qualitative assay (2). The resulting relative affinities were E345K > E345Q > E345(WT) for PI(3,4,5)P_3, and the same order E345K > E345Q > E345(WT) for PI(4,5)P_2. These trends matched those previously observed for AKT1 PH domain, namely E17K > E17Q > E17(WT) for both PI(3,4,5)P_3 and PI(4,5)P_2 (2). Thus, as predicted by the sentry glutamate hypothesis and previously noted for AKT1 PH domain (2), side chains of different charge at the putative GRP1 sentry position alter the PIP lipid affinity in the simple fashion expected for direct electrostatic interaction with a negatively charged headgroup. Relative to the neutral sentry glutamine, the negatively charged glutamate lowers affinity for the anionic PIP lipid, while the positively charged lysine increases affinity for PIP lipid.

To more rigorously test the predictions and generality of the sentry glutamate hypothesis, the remainder of the present study focused on the native E345(WT) and E345K GRP1 PH domains. These two domains exhibit opposite extremes of PIP lipid affinity; moreover, E345K is analogous to the well characterized, disease-linked AKT1 E17K mutation. The sentry glutamate hypothesis proposes the native E345 residue plays a key role in maintaining specific PI(3,4,5)P_3 targeting in cells by reducing affinity for constitutive plasma membrane PI(4,5)P_2 (2, 31). The hypothesis therefore predicts that the E345K mutation, by significantly increasing the affinity for PI(4,5)P_2, will enable the mutant protein to bind constitutively to plasma membrane in resting cells. Further experiments were carried out to quantitate the PI(3,4,5)P_3 and PI(4,5)P_2 affinities of E345(WT) and E345K GRP1 PH domains *in vitro*, and to compare their plasma membrane targeting in cells. As these experiments proceeded it became clear that Arf6 binding contributed significantly to GRP1 PH domain targeting in cells as previously reported (24, 25), thus the E345K/I307A mutant was constructed to clarify the role of Arf6 interactions in the E345K background. Finally, the PI(4,5)P_2-specific PLCδ1 PH domain was included as a control displaying a target lipid preference opposite to that of the PI(3,4,5)P_3-specific E345(WT) GRP1 PH domain (7, 30, 32, 33). Figure 1 shows the locations in the GRP1 PH domain structure of the E345 and I307 positions targeted for mutation, and of the bound PI(3,4,5)P_3 headgroup (inositol-1,3,4,5-P_4, or IP_4).

E345K Mutation Enhances GRP1 PH Domain Affinity for Both PI(4,5)P_2 and PI(3,4,5)P_3, with Important Implications for Target Lipid Specificity

A competitive displacement assay previously developed in our laboratory (13) was used to quantify the affinities of PH domains for PI(3,4,5)P_3 and PI(4,5)P_2 in sonicated unilamellar membrane vesicles. The competitive displacement assay enables determination of equilibrium dissociation constants for membrane-bound target lipids in the range 0.1 to 10,000 nM, well-suited for measuring the nanomolar affinity of native GRP1 PH domain for target lipid PI(3,4,5)P_3 in bilayers composed of seven lipids mimicking the lipid composition of the plasma membrane inner leaflet (Table 1) (2). The first step of the assay measured the dissociation constant $K_D(IP_6)$ for PH domain binding to the competitive inhibitor inositol hexakisphosphate (IP_6) in solution by titrating inhibitor into a sample of free PH domain while monitoring the increase in intrinsic tryptophan fluorescence triggered by inhibitor binding (Eq. 1 in Methods). The second step measured the apparent inhibition constant $K_I(IP_6)$ for competitive displacement of the PH domain from membrane-associated PIP lipid by titrating inhibitor into a suspension of PH domains bound to vesicles while monitoring the decrease in protein-to-membrane FRET (Eq. 2). Finally, the standard equation for competitive inhibition (Eq. 3) was used to calculate the dissociation constant $K_D(PIP_n)$ for PH domain binding to the membrane-associated target lipid.

Figure 2 summarizes the equilibrium titrations for (i) the native, wild type GRP1 PH domain, WT; (ii) the single mutant PH domain, E345K; and (iii) the double mutant PH domain, E345K/I307A. Shown for each mutant are both the titration quantifying competitive inhibitor IP_6 binding to free PH domain (Figs. 2A–C) and the titration quantifying competitive displacement of PH domain from membrane-associated PI(3,4,5)P_3 or PI(4,5)P_2 (Fig. 2D–F) by IP_6. Table 2 summarizes the resulting equilibrium constants $K_D(IP_6)$, $K_I(IP_6)$, and $K_D(PIP_n)$ for the three GRP1 PH domains, as well as for the PLCδ1 PH domain (titrations not shown).

Comparison of the equilibrium dissociation constants for competitive inhibitor IP_6 reveals that the E345K mutation significantly increases the affinity of the free GRP1 PH domain for IP_6. Thus, the free E345K domain exhibits a nearly 5-fold higher IP_6 affinity than the WT domain ($K_D(IP_6)$ of 4.1 ± 0.1 μM and 20 ± 3 μM, respectively). By contrast, the I307A mutation at the Arf6 interaction site has little or no effect on inhibitor binding, such that the IP_6 affinity of the E345K/I307A mutant ($K_D(IP_6)$ of 8 ± 2 μM) is within 2-fold that of E345K.

Comparison of the equilibrium dissociation constants for PH domain binding to PI(3,4,5)P_3 or PI(4,5)P_2 embedded in the plasma membrane-like bilayer reveals that the E345K mutation significantly increases the affinity of GRP1 PH domain for both of these PIP lipids (Table 2). The native WT domain binds its membrane-associated target PI(3,4,5)P_3 with high affinity (K_D of 14 ± 8 nM) and binds membrane-bound PI(4,5)P_2 over 200-fold more weakly (K_D of 3000 ± 2000 nM). At the opposite extreme, the PLCδ1 PH domain binds its target PI(4,5)P_2 with a relatively high affinity (K_D of 150 ± 20 nM) while exhibiting much weaker affinity for PI(3,4,5)P_3 ($K_D > 10^4$ nM). In GRP1 PH domain, the E345K charge reversal mutation yields 8-fold greater affinity for the native target PI(3,4,5)P_3 (K_D of 1.7 ± 0.1 nM) relative to WT (Table 2). Strikingly, the E345K mutation also generates a nearly 8-fold higher affinity for PI(4,5)P_2 (K_D of 400 ± 50 nM) compared to WT (Table 2), yielding a PI(4,5)P_2 affinity within 2.6-fold that of the PLCδ1 PH domain (Table 2). Since the latter domain is widely used as a PI(4,5)P_2 sensor and binds to constitutive plasma membrane PI(4,5)P_2 in cells, the E345K mutant is expected to target constitutively to plasma membrane. Finally, the Arf6 interaction mutant E345K/I307A exhibits PI(3,4,5)P_3 and PI(4,5)P_2 affinities (K_D of 1.7 ± 0.7 and 800 ± 100 nM, respectively) that are indistinguishable, within a factor of 2, of the corresponding PI(3,4,5)P_3 and PI(4,5)P_2

affinities observed for the E345K mutant (Table 2). It follows that, in the absence of Arf6, the I307A mutation has little effect on binding of the E345K mutant to target lipids.

Kinetic Analysis Reveals that E345K Triggers PIP Lipid Affinity Increases Primarily by Slowing Off-Rates

In principle, the E345K mutation could increase the equilibrium affinities of GRP1 PH domain for $PI(3,4,5)P_3$ and $PI(4,5)P_2$ by speeding association kinetics or slowing dissociation kinetics. To resolve these possibilities, where feasible the on- and off-rates were measured for the wild type and E345K mutant PH domains binding to membrane-embedded $PI(3,4,5)P_3$ and $PI(4,5)P_2$ by stopped-flow fluorescence, using protein-to-membrane FRET to monitor membrane association or dissociation. Such kinetic measurements were straightforward for the interaction of wild type and E345K domains with $PI(3,4,5)P_3$, since both proteins bind this lipid tightly. (Kinetic parameters could not be determined for wild type protein binding to $PI(4,5)P_2$ due to the low affinity).

Association reactions were carried out by rapidly mixing the free PH domain with target membranes then monitoring the approach-to-equilibrium. Under the saturating conditions employed, the off-rate is negligible and the approach-to-equilibrium yields the true on-rate. Figure 3A and Table 2 show that all three of the GRP1 PH domains, regardless of whether they lack or possess the E345K mutation or the I307A Arf6 interaction mutation, exhibit similar on-rates for $PI(3,4,5)P_3$ within a narrow 2.5-fold range (k_{on} from $(14 \pm 1) \times 10^6\ M^{-1}\ s^{-1}$ to $(35 \pm 1) \times 10^6\ M^{-1}\ s^{-1}$). Moreover, the on-rates of the E345K mutant and the E345K/I307A double mutant for both $PI(3,4,5)P_3$ and $PI(4,5)P_2$ fall within a similar 3-fold range (k_{on} from $(20 \pm 1) \times 10^6\ M^{-1}\ s^{-1}$ to $(53 \pm 1) \times 10^6\ M^{-1}\ s^{-1}$, Table 2). The observed similarities in the measurable on-rates of GRP1 PH domains for $PI(3,4,5)P_3$ and $PI(4,5)P_2$ likely arise from the rate-determining electrostatic search mechanism that the PH domain is known to employ to find its rare target lipid, since this search mechanism relies on interactions between the protein and background PS lipids (13, 34). Such PS-based searching is expected to yield similar on-rates for different PIP target lipids as long as they are present at similar mole percents, as in the present study where $PI(3,4,5)P_3$ and $PI(4,5)P_2$ were always 2 mole percent, and PS was always 21 mole percent.

Dissociation reactions were carried out by stopped-flow mixing pre-formed PH domain–membrane complexes with excess competitive inhibitor, IP_6, thereby ensuring that membrane dissociation is essentially irreversible. As shown in Figure 3A (IV) the E345K mutation slows the dissociation of GRP1 PH domain from $PI(3,4,5)P_3$-containing membranes by a factor of 18-fold relative to wild type (k_{off} of $0.042 \pm 0.007\ s^{-1}$ and $0.79 \pm 0.01\ s^{-1}$, respectively) (Table 2). The rate of dissociation of the E345K mutant from $PI(4,5)P_2$ is well within the measurable range, but is 540-fold faster than its dissociation from $PI(3,4,5)P_3$ (k_{off} of $23 \pm 1\ s^{-1}$ and $0.042 \pm 0.007\ s^{-1}$, respectively) (Table 2). Interestingly, the E345K mutant exhibits a $PI(4,5)P_2$ off-rate nearly the same, within 1.5-fold, as that of PLCδ1 PH domain (k_{off} of $23 \pm 1\ s^{-1}$ and $15 \pm 1\ s^{-1}$, respectively), helping to explain the similar $PI(4,5)P_2$ affinities of the two PH domains (Table 2). The effect of I307A on the dissociation kinetics of the E345K mutant is minimal, such that the E345K/I307A off-rates for $PI(3,4,5)P_3$ and $PI(4,5)P_2$ are within 3.8-fold of the corresponding E345K off-rates (Table 2).

Wherever possible, the measured on- and off- rate constants were used to calculate a kinetic dissociation constant for each protein-target lipid combination ($K_D(PIP_n) = k_{off}/k_{on}$). As shown in Table 2, the K_D values calculated from kinetic constants are within 4-fold of the K_D values measured in equilibrium studies. Such good agreement validates both the equilibrium and kinetic measurements.

Examination of the on- and off-rate constants of the E345K mutant reveals that its higher affinity for $PI(3,4,5)P_3$ over $PI(4,5)P_2$ arises primarily from a 540-fold slower $PI(3,4,5)P_3$ off-rate. Notably, however, the major functional difference between wild type GRP1 PH domain and the E345K mutant (see cell studies below) arises from the increased affinity of the mutant for $PI(4,5)P_2$. While it is not possible to directly determine the kinetic mechanism of this 8-fold affinity increase due to inability to measure the WT $PI(4,5)P_2$ on-rate, the $PI(4,5)P_2$ on-rates of the wild type and E345K PH domains are likely to be similar. Recall that the $PI(3,4,5)P_3$ on-rates of wild type and E345K, as well as the $PI(3,4,5)P_3$ and $PI(4,5)P_2$ on-rates of the E345K and E345K/I307A mutants, are all similar owing to the rate limiting electrostatic search mechanism (see above). Assuming the WT $PI(4,5)P_2$ on-rate falls in the same range due to its standard rate-limiting search process, it would follow that the 8-fold higher affinity of the E345K mutant for $PI(4,5)P_2$ arises from an approximately 8-fold slower dissociation from $PI(4,5)P_2$ relative to WT.

Together the *in vitro* equilibrium and kinetic studies indicate the E345K putative sentry glutamate mutation in GRP1 PH domain behaves similarly to the oncogenic, E17K sentry glutamate mutation in AKT1 PH domain that we characterized previously (2). In both the E345K GRP1 and the E17K AKT1 PH domain mutants, the glutamate to lysine charge reversal mutation significantly increases both the $PI(3,4,5)P_3$ and $PI(4,5)P_2$ affinities. Notably, the resulting $PI(4,5)P_2$ affinity of E345K GRP1 PH domain, like that of E17K AKT1 PH domain, is remarkably similar to the $PI(4,5)P_2$ affinity of PLCδ1 PH domain – the standard $PI(4,5)P_2$ sensor employed in many *in vitro* and live cell studies (2, 30). It was previously observed that the E17K AKT1 PH domain is bound to plasma membrane in the absence of a $PI(3,4,5)P_3$ signal (1) due to its interaction with $PI(4,5)P_2$ (2). The present *in vitro* evidence led us to predict that the E345K GRP1 PH domain would display a similar constitutive targeting to plasma membrane $PI(4,5)P_2$ in resting cells.

Live Cell Studies Confirm the GRP1 E345K PH Domain is Targeted to the Plasma Membrane by $PI(4,5)P_2$

Live cell imaging was used to visualize the intracellular targeting patterns of the PH domains studied *in vitro* while varying the plasma membrane levels of $PI(3,4,5)P_3$ and $PI(4,5)P_2$. Each PH domain was fused at its N-terminus to citrine fluorescent protein (Cit), expressed in serum-starved NIH 3T3 fibroblasts, and imaged in live cells by wide field fluorescence microscopy. Resting cells were serum-starved to minimize stimulation by attractants and growth factors in the media, ensuring low basal plasma membrane levels of the signaling lipid $PI(3,4,5)P_3$.

Figure 4A summarizes the cellular distributions of PH domains in resting cells, and in activated cells with high levels of plasma membrane $PI(3,4,5)P_3$. In resting cells, the wild type GRP1 PH domain fusion Cit–WT is cytoplasmic with no detectable plasma membrane binding (Fig 4A, B). In contrast, the E345K mutant fusion protein Cit–E345K is significantly targeted to plasma membrane, consistent with its increased *in vitro* affinity for constitutive plasma membrane $PI(4,5)P_2$ (Fig. 4A, B; Table 2). As expected, the PLCδ1 PH domain is also targeted to plasma membrane in resting cells due to its high affinity for constitutive $PI(4,5)P_2$ (Fig. 4A, B; Table 2). Global extracellular addition of PDGF activates phosphatidylinositol-3-kinase (PI3K) and generates plasma membrane $PI(3,4,5)P_3$ (35). The resulting $PI(3,4,5)P_3$ signal recruits the wild type PH domain to the plasma membrane, and drives additional plasma membrane recruitment of the E345K mutant (Fig. 4A). The observed $PI(3,4,5)P_3$-stimulated recruitment of the wild type and E345K PH domains to plasma membrane is consistent with the high $PI(3,4,5)P_3$ affinities observed for both domains *in vitro* (Table 2). The E345K/I307A mutant behaves similarly to the E345K mutant, exhibiting both detectable plasma membrane binding in resting cells (Fig. 4A, B) and enhanced membrane targeting during a $PI(3,4,5)P_3$ signal (Fig. 4A).

To directly test the hypothesis that the E345K mutant targets to plasma membrane PI(4,5)P_2 in resting cells, Ca^{2+} and ionomycin were added globally to increase cytoplasmic Ca^{2+} and activate PLCδ1 hydrolysis, thereby destroying the plasma membrane PI(4,5)P_2 (29, 30). Figure 4B shows the effect of the resulting PI(4,5)P_2 loss on the cellular distribution of each PH domain. The Ca^{2+}-ionomycin treatment fully relocates the PLCδ1 PH domain from the plasma membrane to the cytoplasm, confirming that the treatment destroys the PI(4,5)P_2 lipid this domain targets (Fig. 4B). By contrast, the treatment only partially relocates the E345K domain to the cytoplasm (Fig. 4B) unless the I307A mutation is known to weaken the PH domain-Arf6 interaction (24, 25) is present. Thus, the E345K/I307A double mutant is fully relocated to cytoplasm by the Ca^{2+}-ionomycin treatment (Fig. 4B). These observations demonstrate that PI(4,5)P_2 binding and Arf6 interactions both make important contributions to the plasma membrane affinity and bound state lifetime of the E345K mutant, consistent with the previous conclusion that native GRP1 PH domain is a dual PI(3,4,5)P_3 and Arf6 sensor (24, 25).

Overall, the live cell findings strongly support the conclusion that the E345K sentry glutamate mutation in GRP1 PH domain, like the corresponding E17K mutation in AKT1 PH domain, drives constitutive plasma membrane targeting via enhanced affinity for PI(4,5)P_2. As a result, the E345K GRP1 PH domain, like the E17K AKT1 PH domain, localizes to plasma membrane even in resting cells lacking a PI(3,4,5)P_3 signal.

Discussion

The present study extends our previous analysis of the molecular mechanism of the E17K mutation in AKT1 PH domain to the analogous E345K mutation in GRP1 PH domain (2). Together, these two studies strongly support the conclusion that a sentry glutamate adjacent to the PI(3,4,5)P_3 binding pocket plays a crucial role in reducing the affinities of both PH domains for constitutive plasma membrane PI(4,5)P_2, thereby ensuring that PH domain recruitment to plasma membrane occurs only during a PI(3,4,5)P_3 signal. Like the AKT1 E17K mutation, the GRP1 E345K mutation at the sentry glutamate position (i) increases the affinity for soluble IP_6 and for membrane-bound PI(3,4,5)P_3 and PI(4,5)P_2 *in vitro*, (ii) yields a PI(4,5)P_2 affinity *in vitro* similar to that of PLCδ1 PH domain, the prototypical PI(4,5)P_2 sensor, and (iii) yields binding to constitutive plasma membrane PI(4,5)P_2 in resting cells, as observed for control PLCδ1 PH domain but not for WT GRP1 PH domain.

The constitutive plasma membrane targeting observed for the sentry glutamate mutants AKT1 E17K and GRP1 E345K arises from their increased PI(4,5)P_2 affinities, and not from their increased PI(3,4,5)P_3 affinities. Thus, in resting cells, starvation to minimize growth factors in the media, thereby suppressing plasma membrane PI(3,4,5)P_3, does not block the constitutive plasma membrane targeting of either PH domain mutant ((2) and Fig. 4, this article). Instead, *in vitro* binding measurements reveal that the PI(4,5)P_2 affinities of AKT1 E17K and GRP1 E345K PH domains are raised to a level sufficient to bind the constitutive plasma membrane PI(4,5)P_2 in resting cells, like the PLCδ1 PH domain ((2) and Table 2). The AKT1 E17K mutation increases the PH domain PI(4,5)P_2 affinity at least 80-fold, from a native $K_D > 10^4$ nM to a K_D of 130 ± 30 nM for the mutant, indistinguishable from the PI(4,5)P_2 affinity of PLCδ1 PH domain (2). The GRP1 E345K mutation increases PI(4,5)P_2 affinity approximately 8-fold, yielding a K_D of 400 ± 50 nM *in vitro* (Table 2), again similar to the PI(4,5)P_2 affinity of PLCδ1 PH domain. Moreover, in cells the PI(4,5)P_2 affinity of GRP E345K PH domain is expected to be further enhanced by interactions with plasma membrane-associated Arf6 ((24, 25) and below). Confirming this picture, the constitutively plasma-membrane targeted AKT1 E17K, GRP1 E345K and PLCδ1 PH domains are displaced from the plasma membrane upon introduction of high cytoplasmic [Ca^{2+}] to activate phospholipase C activity and thereby hydrolyze the PI(4,5)P_2 pool ((2) and Fig.

4B), although the GRP1 E345K PH domain is fully displaced by $PI(4,5)P_2$ hydrolysis only when its interaction with Arf6 is weakened by incorporation of the I307A mutation (Fig. 4B). In short, the evidence indicates that the primary physiological role of the native sentry glutamate of AKT1 and GRP1 is to minimize binding to constitutive plasma membrane $PI(4,5)P_2$ in resting cells. Secondarily, the sentry glutamate also reduces the effective $PI(3,4,5)P_3$ affinity, and this affinity tuning could further optimize cellular responses to $PI(3,4,5)P_3$ signals.

More broadly, the present findings have widespread implications for $PI(3,4,5)P_3$-specific PH domains. Currently, there are seven $PI(3,4,5)P_3$-specific PH domains for which structures are available bound to the $PI(3,4,5)P_3$ headgroup. Figure 5 illustrates the confirmed sentry glutamates of AKT1 (E17, PDB 1H10 (27)) and GRP1 (E345, PDB 1FGY and 1FHX (18, 26)) PH domains, and shows that the other five known structures also possess a putative sentry glutamate (or, in two cases, a putative sentry aspartate): (i) Bruton's tyrosine kinase (BTK, E41, PDB 1B55 (36)); (ii) Arf nucleotide-binding-site opener (ARNO, E341, PDB 1U27 (37)); (iii, iv) centaurin α1 PH1 and PH2 (CENTA1, D142 and E268, respectively, PDB 3LJU(38)); and (v) 3-phosphanositide-dependent kinase 1 (PDK1, D488, PDB 1W1D (39)). It follows that an acidic sentry side chain is a common, perhaps ubiquitous, feature of $PI(3,4,5)P_3$-specific PH domains. However, these acidic sentry residues may have arisen from convergent evolution, since their locations in the PH domain architecture are not conserved. Examination of Figure 5 reveals that the proposed sentry residues are distributed among different loops and are disposed differently relative to the $PI(3,4,5)P_3$ headgroup. In five cases (AKT1, GRP1, ARNO, CENTA1 PH1 and PH2) the sentry side chain carboxylate is predicted to have the strongest repulsive electrostatic interaction with the 5-phosphate of the $PI(3,4,5)P_3$ headgroup due to proximity or, in certain cases, due to screening of other proximal phosphates by intervening basic side chains. In the remaining cases (BTK, PDK1) the side chain carboxylate is predicted to interact most strongly with the 1-phosphate.

The different locations of sentry glutamates are likely to yield subtle mechanistic differences as illustrated by a comparison of AKT1 and GRP1. In both cases, the mobile side chain carboxylate of the sentry glutamate can closely approach the 5-phosphate, but AKT E17 is on loop β1/β2 (27) and GRP1 E345 is on loop β6/β7 (18) on opposite sides of the inositol ring. The E17K AKT1 PH domain mutation increases the $PI(3,4,5)P_3$ affinity by a factor of 8-fold, and increases the affinity for $PI(4,5)P_2$ by a much greater 80-fold factor. By contrast, the E345K GRP1 PH domain mutation increases the affinity for both $PI(3,4,5)P_3$ and $PI(4,5)P_2$ by the same factors of 8-fold. The simplest explanation for the more dramatic effect of the E17K mutation on $PI(4,5)P_2$ affinity is that the sentry glutamate of AKT1 PH domain prevents the binding of the $PI(4,5)P_2$ headgroup in an alternative orientation that would yield significantly tighter binding, while this alternative $PI(4,5)P_2$ orientation is not accessible in GRP1 PH domain.

The strikingly similar, 8-fold affinity increases observed for the interactions of E17K AKT1 PH domain with $PI(3,4,5)P_3$, and for GRP1 PH domain with both $PI(3,4,5)P_3$ and $PI(4,5)P_2$, may share similar mechanisms. In principle, at least three electrostatic interactions could be involved, but only one is favored by the data. (i) In crystal structures of the apo state, the AKT1 or GRP1 sentry glutamate forms a salt bridge to a nearby basic side chain required for PIP headgroup coordination (E17 to K14 and E345 to R349, respectively). This salt bridge must be broken for the PIP headgroup to bind, yielding an energy barrier for binding that is eliminated by the E17K or E345K mutation. However, the kinetic analysis indicates this barrier is insignificant since the measured target lipid on-rates (Table 2) are largely unaffected by the sentry mutations. The findings are consistent with the previously documented rate-determining, electrostatic search process that involves membrane-embedded PS and defines the target lipid association kinetics (13, 34). It follows that an apo-

state salt bridge does not play a central role in sentry glutamate function. (ii) When bound to its target lipid on the membrane surface, the AKT1 or GRP1 PH domain interacts electrostatically with negatively charged lipids, primarily phosphatidylserine (PS). This interaction would be repulsive for the native sentry glutamate, but the E17K or E345K mutation would convert this repulsive interaction into an attractive interaction, thereby stabilizing the bound state and increasing target lipid affinity. Such a picture is disfavored by the observation that a membrane is not required for the affinity increase, since both mutations trigger affinity increases for soluble IP_6 similar in magnitude to the affinity increases observed for membrane-embedded PIP lipids ((2) and Table 2). (iii) Instead, the molecular basis of sentry function appears to be the electrostatic interaction between the sentry side chain carboxylate and the PIP lipid headgroup. The sentry glutamate side chain is presumably dynamic, and the AKT1 and GRP1 co-crystal structures with a $PI(3,4,5)P_3$ headgroup analogue both indicate the side chain carboxylate can approach the inositol 5-phosphate of the target headgroup well within the ~ 8 Å Debye limit for significant electrostatic interactions at physiological ionic strength. The resulting carboxylate-phosphate charge repulsion would generate an energy barrier for PIP headgroup binding that would be converted to a favorable electrostatic interaction by the E17K or E345K mutation. This picture explains the higher $PI(3,4,5)P_3$, $PI(4,5)P_2$ and IP_6 affinities observed for the AKT1 and GRP1 sentry lysine mutants, as well as the slower $PI(3,4,5)P_3$ dissociation kinetics observed for these mutants ((2) and Table 2).

Thus, the native sentry glutamate is a negative regulator of $PI(4,5)P_2$ binding, and charge reversal to lysine enhances both the $PI(4,5)P_2$ and $PI(3,4,5)P_3$ affinities. These observations may provide a clue to the evolution of $PI(3,4,5)P_3$-specific PH domains. If ancestor cells possessed sufficiently low constitutive levels of $PI(4,5)P_2$ and generated smaller $PI(3,4,5)P_3$ signals, the original PH domains may have required lysine or arginine residues at the position now occupied by the sentry glutamate. Modern $PI(3,4,5)P_3$-specific PH domains that encounter high levels of $PI(4,5)P_2$, however require the sentry glutamate to ensure that plasma membrane targeting occurs only during a $PI(3,4,5)P_3$ signal. The glutamate also moderates the high $PI(3,4,5)P_3$ affinity generated by the multiple basic residues that coordinate the $PI(3,4,5)P_3$ in the headgroup binding pocket. In the case of GRP1 PH domain, one of these residues is a His sidechain (His 355) that may further modulate $PI(3,4,5)P_3$ targeting by introducing a strong pH sensitivity (40).

The physiological impact of the glutamate to lysine charge reversal mutation at the sentry glutamate position has been previously demonstrated for full length AKT1 E17K, since this mutant is an oncogenic kinase ((1, 41) and recently confirmed in (42)). The constitutive plasma membrane targeting of AKT1 E17K leads to hyperactivation of its kinase activity, transformation of tissue culture cells, multiple human cancers and, in the case of Proteus syndrome, tissue overgrowth (1, 3). Similarly, while the BTK E41 residue has not been directly confirmed as a sentry glutamate due to lack of quantitative equilibrium and kinetic analysis, the BTK E41K mutation does lead to $PI(4,5)P_2$ binding *in vitro* as well as constitutive targeting to plasma membrane and transformation of tissue culture cells (36, 43, 44). Thus, the available evidence suggests that BTK E41 is likely a sentry glutamate and its primary role is to minimize $PI(4,5)P_2$ binding in resting cells, as demonstrated for AKT1 E17 and GRP1 E345. While to date only the AKT1 E17K mutation has been directly linked to disease, the ability of charge reversal mutations at sentry glutamate positions to trigger constitutive plasma membrane targeting suggests that future studies may well uncover diseases linked to the GRP1 E345K or BTK E41K mutation, or to sentry charge reversals in other PH domains.

Acknowledgments

†Support provided by NIH R01 GM-063235 (to JJF) and NIH T32 GM-065103 (to KEL)

The authors thank Drs. Amy Palmer for technical advice on cell imaging, Brian Ziemba for critical reading of the manuscript, and *Biochemistry* reviewers for helpful suggestions.

Abbreviations

AKT1	protein kinase B, isoform 1
PDK1	phosphoinositide dependent protein kinase 1
PLCδ-1	phospholipase C delta, isoform 1
PH	pleckstrin homology
PC	phosphatidylcholine
PS	phosphatidylserine
PE	phosphatidylethanolamine
dPE	dansyl-PE
PI(3,4,5)P_3	phosphatidylinositol-3,4,5-trisphosphate
PI(4,5)P_2	phosphatidylinositol-4,5-bisphosphate
DTT	dithiothreitol
IP_6	inositol-hexakisphosphate

References

1. Carpten JD, Faber AL, Horn C, Donoho GP, Briggs SL, Robbins CM, Hostetter G, Boguslawski S, Moses TY, Savage S, Uhlik M, Lin A, Du J, Qian YW, Zeckner DJ, Tucker-Kellogg G, Touchman J, Patel K, Mousses S, Bittner M, Schevitz R, Lai MH, Blanchard KL, Thomas JE. A transforming mutation in the pleckstrin homology domain of AKT1 in cancer. Nature. 2007; 448:439–444. [PubMed: 17611497]
2. Landgraf KE, Pilling C, Falke JJ. Molecular mechanism of an oncogenic mutation that alters membrane targeting: Glu17Lys modifies the PIP lipid specificity of the AKT1 PH domain. Biochemistry. 2008; 47:12260–12269. [PubMed: 18954143]
3. Lindhurst MJ, Sapp JC, Teer JK, Johnston JJ, Finn EM, Peters K, Turner J, Cannons JL, Bick D, Blakemore L, Blumhorst C, Brockmann K, Calder P, Cherman N, Deardorff MA, Everman DB, Golas G, Greenstein RM, Kato BM, Keppler-Noreuil KM, Kuznetsov SA, Miyamoto RT, Newman K, Ng D, O'Brien K, Rothenberg S, Schwartzentruber DJ, Singhal V, Tirabosco R, Upton J, Wientroub S, Zackai EH, Hoag K, Whitewood-Neal T, Robey PG, Schwartzberg PL, Darling TN, Tosi LL, Mullikin JC, Biesecker LG. A mosaic activating mutation in AKT1 associated with the Proteus syndrome. N Engl J Med. 2011; 365:611–619. [PubMed: 21793738]
4. Vanhaesebroeck B, Leevers SJ, Ahmadi K, Timms J, Katso R, Driscoll PC, Woscholski R, Parker PJ, Waterfield MD. Synthesis and function of 3-phosphorylated inositol lipids. Annu Rev Biochem. 2001; 70:535–602. [PubMed: 11395417]
5. Hawkins PT, Anderson KE, Davidson K, Stephens LR. Signalling through Class I PI3Ks in mammalian cells. Biochemical Society Transactions. 2006; 34:647–662. [PubMed: 17052169]
6. Newton AC. Lipid activation of protein kinases. J Lipid Res. 2009; 50(Suppl):S266–271. [PubMed: 19033211]
7. Lemmon MA, Ferguson KM. Signal-dependent membrane targeting by pleckstrin homology (PH) domains. Biochem J. 2000; 350(Pt 1):1–18. [PubMed: 10926821]
8. Czech MP. PIP2 and PIP3: complex roles at the cell surface. Cell. 2000; 100:603–606. [PubMed: 10761925]

9. Insall RH, Weiner OD. PIP3, PIP2, and cell movement--similar messages, different meanings? Dev Cell. 2001; 1:743–747. [PubMed: 11740936]
10. Wang F, Herzmark P, Weiner OD, Srinivasan S, Servant G, Bourne HR. Lipid products of PI(3)Ks maintain persistent cell polarity and directed motility in neutrophils. Nat Cell Biol. 2002; 4:513–518. [PubMed: 12080345]
11. Czech MP. Dynamics of phosphoinositides in membrane retrieval and insertion. Annu Rev Physiol. 2003; 65:791–815. [PubMed: 12518000]
12. DiNitto JP, Cronin TC, Lambright DG. Membrane recognition and targeting by lipid-binding domains. Sci STKE. 2003:re16. [PubMed: 14679290]
13. Corbin JA, Dirkx RA, Falke JJ. GRP1 pleckstrin homology domain: activation parameters and novel search mechanism for rare target lipid. Biochemistry. 2004; 43:16161–16173. [PubMed: 15610010]
14. Hennessy BT, Smith DL, Ram PT, Lu Y, Mills GB. Exploiting the PI3K/AKT pathway for cancer drug discovery. Nat Rev Drug Discov. 2005; 4:988–1004. [PubMed: 16341064]
15. Hurley JH. Membrane binding domains. Biochim Biophys Acta. 2006; 1761:805–811. [PubMed: 16616874]
16. Fayard E, Xue G, Parcellier A, Bozulic L, Hemmings BA. Protein kinase B (PKB/Akt), a key mediator of the PI3K signaling pathway. Curr Top Microbiol Immunol. 2010; 346:31–56. [PubMed: 20517722]
17. Finn RD, Mistry J, Tate J, Coggill P, Heger A, Pollington JE, Gavin OL, Gunasekaran P, Ceric G, Forslund K, Holm L, Sonnhammer EL, Eddy SR, Bateman A. The Pfam protein families database. Nucleic Acids Res. 2010; 38:D211–222. [PubMed: 19920124]
18. Lietzke SE, Bose S, Cronin T, Klarlund J, Chawla A, Czech MP, Lambright DG. Structural basis of 3-phosphoinositide recognition by pleckstrin homology domains. Mol Cell. 2000; 6:385–394. [PubMed: 10983985]
19. Park WS, Heo WD, Whalen JH, O'Rourke NA, Bryan HM, Meyer T, Teruel MN. Comprehensive identification of PIP3-regulated PH domains from C. elegans to H. sapiens by model prediction and live imaging. Mol Cell. 2008; 30:381–392. [PubMed: 18471983]
20. Calleja V, Laguerre M, Larijani B. 3-D structure and dynamics of protein kinase B-new mechanism for the allosteric regulation of an AGC kinase. J Chem Biol. 2009; 2:11–25. [PubMed: 19568789]
21. Calleja V, Alcor D, Laguerre M, Park J, Vojnovic B, Hemmings BA, Downward J, Parker PJ, Larijani B. Intramolecular and intermolecular interactions of protein kinase B define its activation in vivo. PLoS Biol. 2007; 5:e95. [PubMed: 17407381]
22. Okuzumi T, Fiedler D, Zhang C, Gray DC, Aizenstein B, Hoffman R, Shokat KM. Inhibitor hijacking of Akt activation. Nat Chem Biol. 2009; 5:484–493. [PubMed: 19465931]
23. Wu WI, Voegtli WC, Sturgis HL, Dizon FP, Vigers GP, Brandhuber BJ. Crystal structure of human AKT1 with an allosteric inhibitor reveals a new mode of kinase inhibition. PLoS One. 2010; 5:e12913. [PubMed: 20886116]
24. Jackson TR, Kearns BG, Theibert AB. Cytohesins and Centaurins: Mediators of PI 3-Kinase Regulated Arf Signaling. Trends Biochem Sci. 2000; 25:489–495. [PubMed: 11050434]
25. Cohen LA, Honda A, Varnai P, Brown FD, Balla T, Donaldson JG. Active Arf6 Recruits ARNO/Cytohesin GEFs to the PM by Binding Their PH Domains. Mol Biol Cell. 2007; 18:2244–2253. [PubMed: 17409355]
26. Ferguson KM, Kavran JM, Sankaran VG, Fournier E, Isakoff SJ, Skolnik EY, Lemmon MA. Structural basis for discrimination of 3-phosphoinositides by pleckstrin homology domains. Mol Cell. 2000; 6:373–384. [PubMed: 10983984]
27. Thomas CC, Deak M, Alessi DR, van Aalten DM. High-resolution structure of the pleckstrin homology domain of protein kinase b/akt bound to phosphatidylinositol (3,4,5)-trisphosphate. Curr Biol. 2002; 12:1256–1262. [PubMed: 12176338]
28. Saxena A, Morozov P, Frank D, Musalo R, Lemmon MA, Skolnik EY, Tycko B. Phosphoinositide binding by the pleckstrin homology domains of Ipl and Tih1. J Biol Chem. 2002; 277:49935–49944. [PubMed: 12374806]

29. Allen V, Swigart P, Cheung R, Cockcroft S, Katan M. Regulation of inositol lipid-specific phospholipase cdelta by changes in Ca2+ ion concentrations. Biochem J. 1997; 327 (Pt 2):545–552. [PubMed: 9359428]
30. van der Wal J, Habets R, Varnai P, Balla T, Jalink K. Monitoring agonist-induced phospholipase C activation in live cells by fluorescence resonance energy transfer. J Biol Chem. 2001; 276:15337–15344. [PubMed: 11152673]
31. Falke JJ. Membrane Recruitment as a Cancer Mechanism: A Case Study of Akt PH Domain. Cell science. 2007; 4:25–30. [PubMed: 19079757]
32. Garcia P, Gupta R, Shah S, Morris AJ, Rudge SA, Scarlata S, Petrova V, McLaughlin S, Rebecchi MJ. The pleckstrin homology domain of phospholipase C-delta 1 binds with high affinity to phosphatidylinositol 4,5-bisphosphate in bilayer membranes. Biochemistry. 1995; 34:16228–16234. [PubMed: 8519781]
33. Singh SM, Murray D. Molecular modeling of the membrane targeting of phospholipase C pleckstrin homology domains. Protein Sci. 2003; 12:1934–1953. [PubMed: 12930993]
34. Knight JD, Falke JJ. Single-molecule fluorescence studies of a PH domain: new insights into the membrane docking reaction. Biophys J. 2009; 96:566–582. [PubMed: 19167305]
35. Toker A, Cantley LC. Signalling through the lipid products of phosphoinositide-3-OH kinase. Nature. 1997; 387:673–676. [PubMed: 9192891]
36. Baraldi E, Djinovic Carugo K, Hyvonen M, Surdo PL, Riley AM, Potter BV, O'Brien R, Ladbury JE, Saraste M. Structure of the PH domain from Bruton's tyrosine kinase in complex with inositol 1,3,4,5-tetrakisphosphate. Structure. 1999; 7:449–460. [PubMed: 10196129]
37. Cronin TC, DiNitto JP, Czech MP, Lambright DG. Structural determinants of phosphoinositide selectivity in splice variants of Grp1 family PH domains. EMBO J. 2004; 23:3711–3720. [PubMed: 15359279]
38. Tong Y, Tempel W, Wang H, Yamada K, Shen L, Senisterra GA, MacKenzie F, Chishti AH, Park HW. Phosphorylation-independent dual-site binding of the FHA domain of KIF13 mediates phosphoinositide transport via centaurin alpha1. Proc Nat Acad Sci USA. 2010; 107:20346–20351. [PubMed: 21057110]
39. Komander D, Fairservice A, Deak M, Kular GS, Prescott AR, Peter Downes C, Safrany ST, Alessi DR, van Aalten DM. Structural insights into the regulation of PDK1 by phosphoinositides and inositol phosphates. EMBO J. 2004; 23:3918–3928. [PubMed: 15457207]
40. He J, Haney RM, Vora M, Verkhusha VV, Stahelin RV, Kutateladze TG. Molecular mechanism of membrane targeting by the GRP1 PH domain. J Lipid Res. 2008; 49:1807–1815. [PubMed: 18469301]
41. Malanga D, Scrima M, De Marco C, Fabiani F, De Rosa N, De Gisi S, Malara N, Savino R, Rocco G, Chiappetta G, Franco R, Tirino V, Pirozzi G, Viglietto G. Activating E17K mutation in the gene encoding the protein kinase AKT1 in a subset of squamous cell carcinoma of the lung. Cell Cycle. 2008; 7:665–669. [PubMed: 18256540]
42. Dannemann N, Hart JR, Ueno L, Vogt PK. Phosphatidylinositol 4,5-bisphosphate-specific AKT1 is oncogenic. Int J Cancer. 2010; 127:239–244. [PubMed: 19876913]
43. Li T, Tsukada S, Satterthwaite A, Havlik MH, Park H, Takatsu K, Witte ON. Activation of Bruton's tyrosine kinase (BTK) by a point mutation in its pleckstrin homology (PH) domain. Immunity. 1995; 2:451–460. [PubMed: 7538439]
44. Varnai P, Rother KI, Balla T. Phosphatidylinositol 3-kinase-dependent membrane association of the Bruton's tyrosine kinase pleckstrin homology domain visualized in single living cells. J Biol Chem. 1999; 274:10983–10989. [PubMed: 10196179]
45. Varnai P, Balla T. Visualization of phosphoinositides that bind pleckstrin homology domains: calcium- and agonist-induced dynamic changes and relationship to myo-[3H]inositol-labeled phosphoinositide pools. J Cell Biol. 1998; 143:501–510. [PubMed: 9786958]

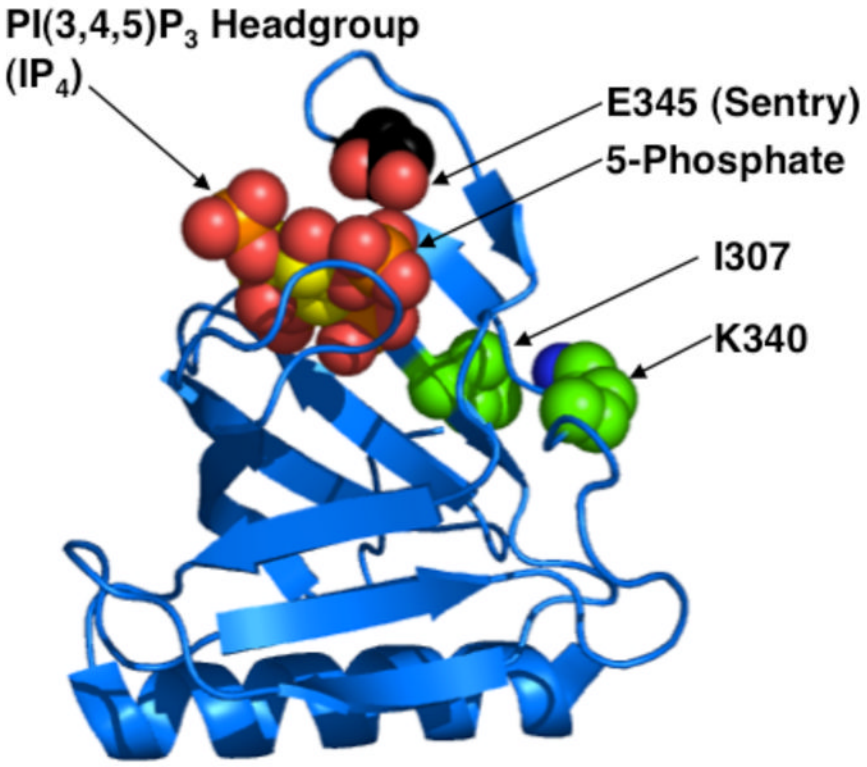

FIGURE 1.
Locations of relevant residues in the crystal structure of GRP1 PH domain (18, 26). The proposed sentry glutamate E345 is located adjacent to binding pocket for PI(3,4,5)P_3 headgroup (IP_4), near the 5-phosphate. The Arf6 docking surface includes residues I307 and K340 (24, 25). The present study employs the E345K charge reversal mutation to test the sentry glutamate hypothesis, and the I307A mutation to weaken the interaction between GRP1 PH domain and Arf6.

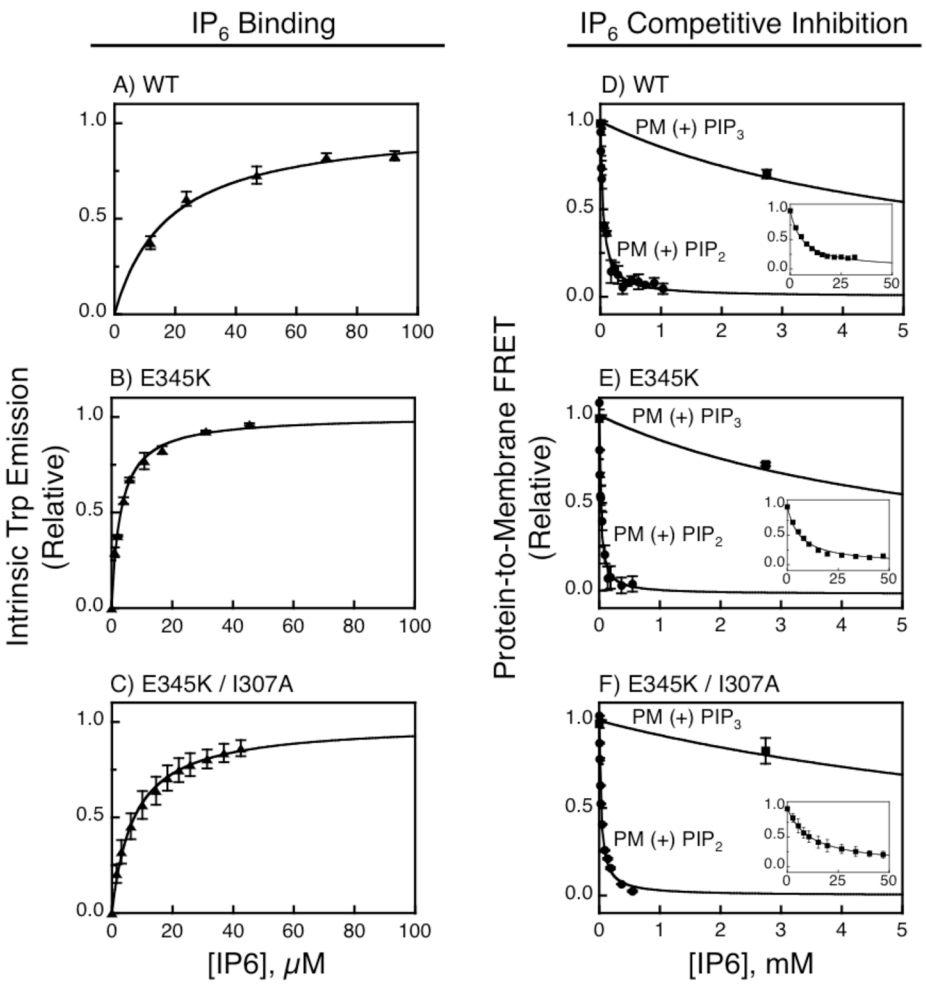

FIGURE 2.

Quantitative equilibrium binding and specificity measurements. (A–C) Direct measurement of IP_6 binding to free PH domain in which 0.5 μM of each protein was titrated with IP_6 while quantitating the increase in tryptophan emission resulting from complex formation (see Methods). (D–F) Competitive displacement assay for the indicated PH domain bound to either PI(3,4,5)P_3 (squares) or PI(4,5,)P_2 (circles) on plasma membrane-like sonicated unilamellar vesicles. To form the protein-membrane complex, protein (0.5 μM) was mixed with target vesicles (300 μM total lipid, 3 μM accessible PIP lipid). Subsequently, protein was displaced from target vesicles by titration with the competitive inhibitor IP_6 while monitoring the decrease in protein-to-membrane FRET (see Methods). In each panel, assays were carried out in triplicate at 25° C in a physiological buffer, data points are averages (±1 standard deviation), and best fit curves were defined by Eq. 1 (A–C) or 2 (D–F). Insets (D–F) show full titration for proteins bound to PI(3,4,5)P_3. Table 2 presents parameters defined by averaging best-fit values defined by three or more independent measurements.

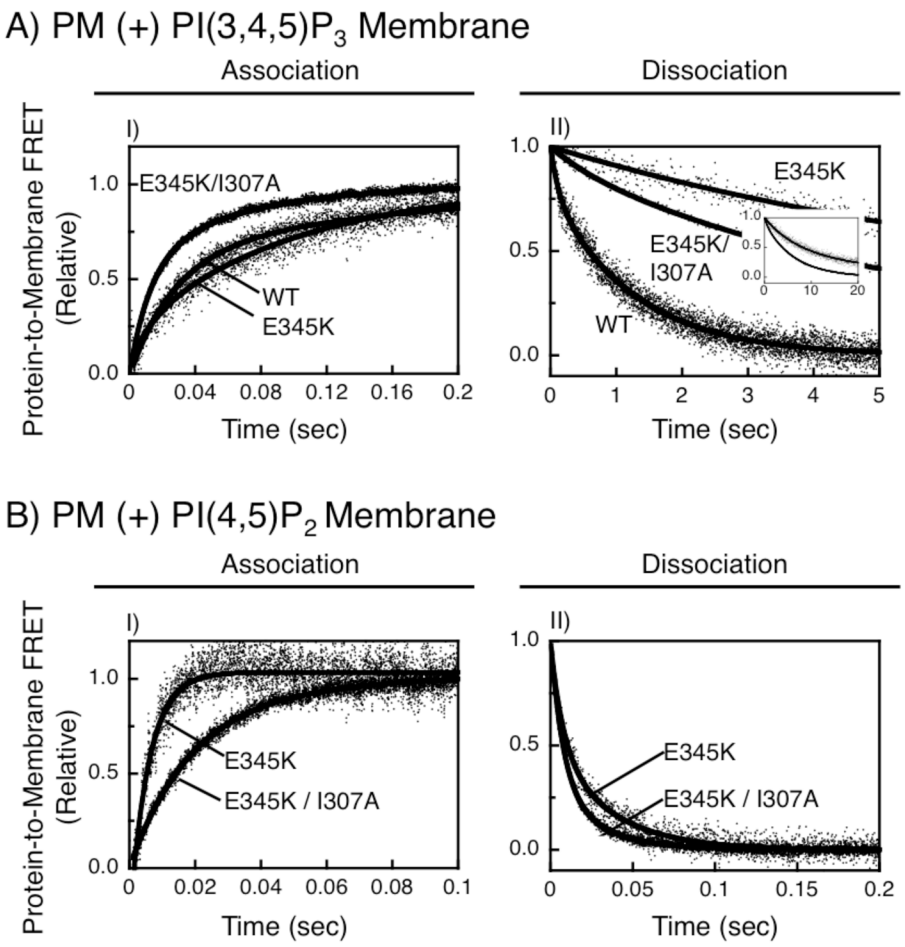

FIGURE 3.

Association and dissociation rate measurements. Shown are association and dissociation reactions of indicated PH domains binding to $PI(3,4,5)P_3$ (A) or $PI(4,5,)P_2$ (B) embedded in plasma membrane-like bilayers. In all cases the final protein and lipid concentrations were identical to the equilibrium competitive displacement assays (Fig. 2). Reactions were initiated by rapid mixing of either the free PH domain with membranes (association) or the prebound PH domain-membrane complex with IP_6 (dissociation) as described in Methods. Note that the time axis is optimized for each panel. For each reaction, at least five shots were carried out at 25º C in a physiological buffer and then averaged to give the representative trace. Bold curves indicate best-fit double exponential functions, which yielded dominant fast (association) and slow (dissociation) components used to determine on- and off-rate constants as previously described (13). For each rate constant, at least 3 independent measurements were averaged to produce the parameters summarized in Table 2. The inset shows the full timecourses of the two mutant dissociation reactions.

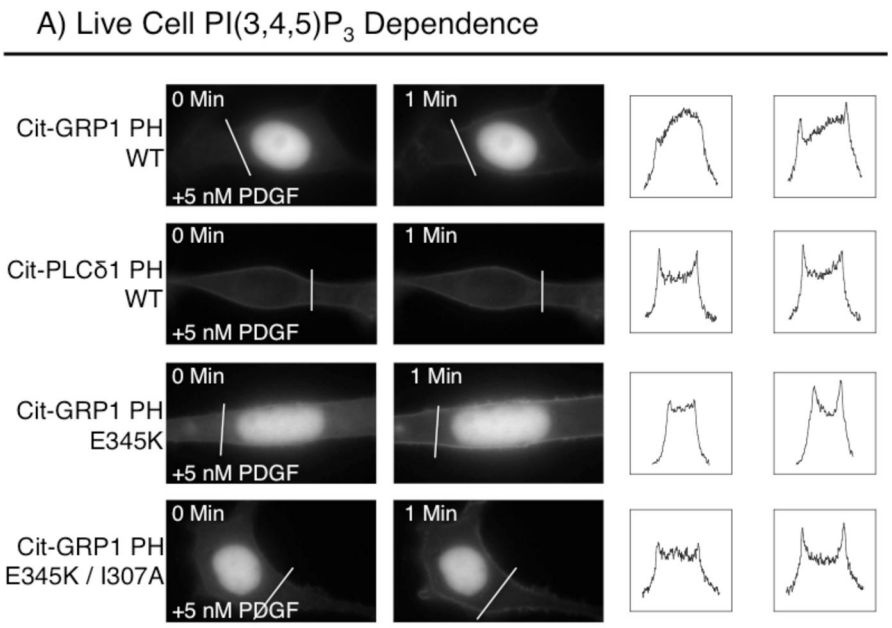

Figure 4A

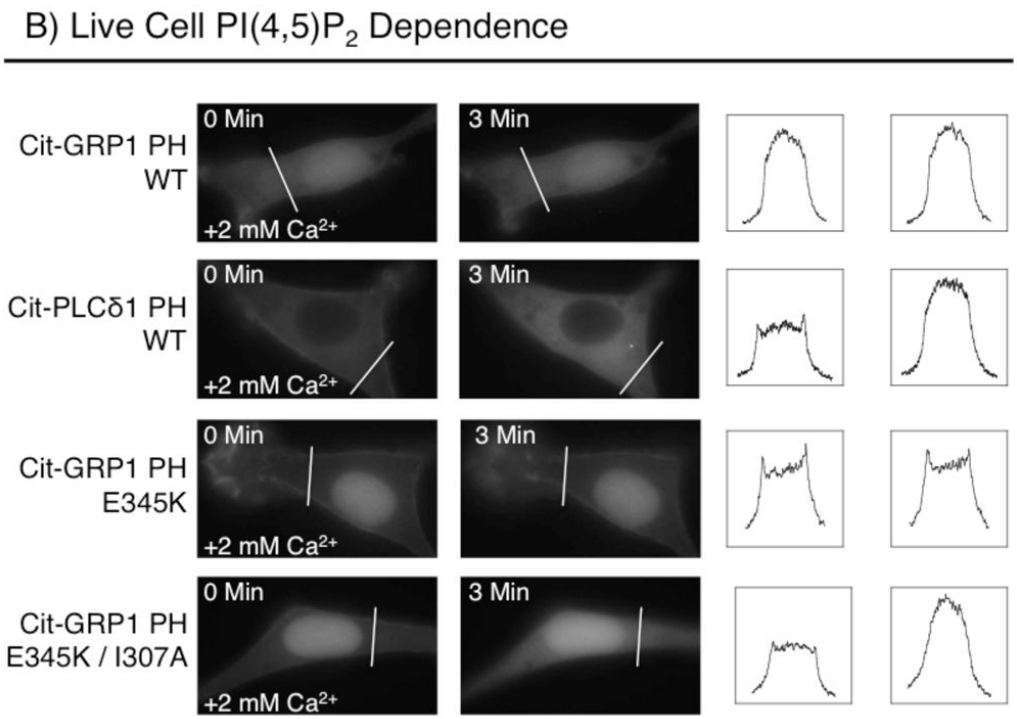

Figure 4B

FIGURE 4.

PIP lipid dependence of plasma membrane targeting in NIH 3T3 cells. (A) Dependence of membrane targeting on $PI(3,4,5)P_3$. Shown are the zero time and one minute images for the indicated citrine-coupled PH domains. Serum-starved NIH 3T3 cells were stimulated with 5 nM PDGF at time zero and imaged at multiple timepoints (see Methods). (B) Dependence of membrane targeting on $PI(4,5)P_2$ for the indicated citrine-coupled PH domains. Shown are the zero time and three minute images for the indicated citrine-coupled PH domains. Serum-starved NIH 3T3 cells were incubated in 20 μM ionomycin in Ca^{2+}-free buffer, then stimulated at time zero with 2 mM extracellular Ca^{2+} to trigger cytoplasmic Ca^{2+} influx and Ca^{2+}-activated $PI(4,5)P_2$ hydrolysis (45) with imaging at multiple timepoints (see Methods). Each set of images are representative examples of responses observed for 12 or more cells. To assist visualization of the protein movements between the plasma membrane and cytoplasm, fluorescence intensities for pixels defined by the indicated line across each cell are plotted for both before (left box) and after (right box) treatment.

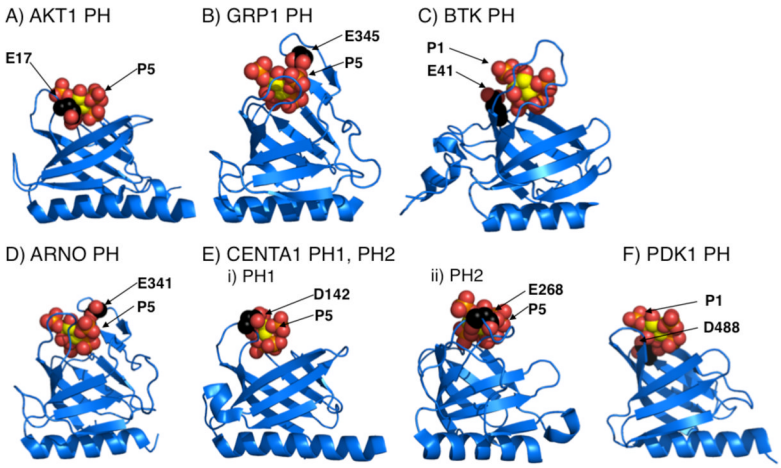

FIGURE 5.

Comparison of all six PI(3,4,5)P_3-specific PH domains for which co-crystal structures with bound PI(3,4,5)P_3 headgroup are currently available (26,17,25,35–38). Highlighted are the putative sentry residue and the headgroup phosphate predicted to have the strongest electrostatic interactions with the sentry side chain carboxylate (see Discussion).

Table 1

Lipid composition of plasma membrane mimics

Name	Lipid Mixture	Lipid mol %
PM(+)PIP_n	PE/PC/PS/PI/SM/CH/dPE/PIP_n	27.5/10.5/21/4.5/4.5/25/5/2
PM	PE/PC/PS/PI/SM/CH/dPE	29.5/10.5/21/4.5/4.5/25/5

Table 2

Equilibrium and Kinetic Parameters for PH domains Binding to Plasma Membrane Mimics Containing PIP Lipids

			Equilibrium		Kinetics		
PH Domain	**$K_D(IP_6)$ (μM)**	**Plasma Membrane Mimic[a]**	**$K_I(IP_6)$ (mM)**	**$K_D(PIP_n)$ (nM)**	**k_{on} ($\times 10^6$ M^{-1} s^{-1})**	**k_{off} (s^{-1})**	**K_D (k_{off}/k_{on}) (nM)**
WT	20 ± 3	PM(+)PI(3,4,5)P_3	5 ± 2	14 ± 8	14 ± 1	0.79 ± 0.01	55 ± 1
		PM(+)PI(4,5)P_2	0.04 ± 0.01	3000 ± 2000	ND[b]	ND[b]	—
E345K	4.1 ± 0.1	PM(+)PI(3,4,5)P_3	7 ± 2	1.7 ± 0.1	20 ± 1	0.042 ± 0.007	2.1 ± 0.3
		PM(+)PI(4,5)P_2	0.026 ± 0.005	400 ± 50	53 ± 1	23 ± 1	430 ± 20
E345K/I307A	8 ± 2	PM(+)PI(3,4,5)P_3	14 ± 4	1.7 ± 0.7	35 ± 1	0.16 ± 0.01	4.6 ± 0.1
		PM(+)PI(4,5)P_2	0.035 ± 0.005	800 ± 100	32 ± 1	18 ± 1	550 ± 20
PLCδ1	4 ± 1	PM(+)PI(3,4,5)P_3	ND[b]	> 10^4[c]	ND[b]	ND[b]	—
		PM(+)PI(4,5)P_2	0.07 ± 0.01	150 ± 20	180 ± 10	15 ± 1	81 ± 5

[a] PIP lipid level is 2 mole percent (Table 1).

[b] Not determined due to insufficient affinity.

[c] Lower limit determined as previously described (2).